

Anisohydric characteristics of a rice genotype ‘ARC 11094’ contribute to increased photosynthetic carbon fixation under fluctuating light conditions

Kazuki Taniyoshi¹, Yu Tanaka¹, Shunsuke Adachi², and Tatsuhiko Shiraiwa¹

¹Kyoto Daigaku Nogaku Kenkyuka Nogakubu

²Tokyo Noko Daigaku Nogakubu Daigakuin Nogaku Kenkyuin

July 11, 2022

Abstract

Photosynthetic induction, which is the response of the CO₂ assimilation rate to a stepwise increase in light intensity, potentially affects plant carbon gain and crop productivity in field environments. Although natural variations in photosynthetic induction are determined by CO₂ supply and its fixation, detailed factors, especially CO₂ supply, are unclear. This study investigated photosynthesis at steady and non-steady states in three rice (*Oryza sativa* L.) genotypes: ARC 11094, Takanari, and Koshihikari. Stomatal traits and water relations in the plants were evaluated to characterise CO₂ supply. Photosynthetic induction was higher in ARC 11094 and Takanari than in Koshihikari owing to an efficient CO₂ supply. The CO₂ supply in Takanari is attributed to its high stomatal density, long guard cell length, and extensive root mass, whereas that in ARC 11094 is attributed to its high stomatal conductance per stoma and stomatal opening in leaves with insufficient water (i.e. anisohydric stomatal behaviour). Our results suggest that there are various mechanisms for realising an efficient CO₂ supply during the induction response. These characteristics can be useful for improving photosynthetic induction and, thus, crop productivity in field environments in future breeding programs.

Introduction

Due to the global population explosion with the increase in food demand, there is a need for improved crop productivity. Photosynthesis is one of the most critical traits for increasing crop productivity (Long *et al.* , 2006; Zhu *et al.* , 2010). In natural environments, light intensity in the plant canopy fluctuates by seconds or minutes because of cloud movements, self-shading, etc. (Percy & Way, 2012). Fluctuating light intensity affects carbon assimilation efficiency and thus plant biomass production (Slattery *et al.* , 2018). Specifically, the CO₂ assimilation rate (A) increases gradually with the sudden increase in the light intensity, and it takes a substantial amount of time to reach a steady-state (Yamori, 2016). This process is called photosynthetic induction (Percy, 1990) and is estimated to cost 21% of potential daily carbon assimilation (Taylor & Long, 2017; Tanaka *et al.* , 2019). Therefore, photosynthetic induction is considered an essential trait for enhancing crop productivity.

During the induction response, mainly two processes, namely, biochemical and stomatal processes, limit photosynthesis. In biochemical processes, Calvin–Benson cycle enzymes and photosynthetic electron transport rates at the thylakoid membrane play crucial roles in CO₂ fixation in the mesophyll cells (Yamori *et al.* , 2012, 2016; Kaiser *et al.* , 2016). In stomatal processes, stomatal conductance (g_s) regulates CO₂ supply from the atmosphere to the carboxylation sites, thereby affecting A during the induction response (Kaiser *et al.* , 2016; Kimura *et al.* , 2020; Yamori *et al.* , 2020).

There are significant natural variations in photosynthetic induction in some crops, such as rice (Acevedo-

Siacca *et al.* , 2020, 2021; Taniyoshi *et al.* , 2020), soybean (Soleh *et al.* , 2017), wheat (Salter *et al.* , 2019), and barley (Salter *et al.* , 2020). Soleh *et al.* . (2016), Taylor and Long (2017), and Salter *et al.* . (2019) revealed that the maximum rate of ribulose 1,5-bisphosphate (RuBP) carboxylation (V_{Cmax}) imposes a significant limitation on A during the induction response. Adachi *et al.* . (2019) described a pool of Calvin–Benson cycle metabolites and showed that photosynthetic electron transport rate responses are essential for photosynthetic induction. The importance of g_s under fluctuating light has also been described previously (Qu *et al.* , 2016; Adachi *et al.* , 2019), but little is known about the factors underlying the natural variation in CO_2 supply.

In general, stomatal opening is attributed to stomatal morphology (Faralli *et al.* , 2019; Zhang *et al.* , 2019; Harrison *et al.* , 2020; Lawson & Matthews, 2020; Xiong *et al.* , 2022), abscisic acid sensitivity (Kaiser *et al.* , 2016) or blue light sensitivity (Papanatsiou *et al.* , 2019; Matthews *et al.* , 2020). Water relations in plants also affect leaf photosynthesis (Hirasawa *et al.* , 1992). Stomatal aperture is observed to close with hydroactive stomatal response when the water potential of the leaf declines (Glinka, 1971; DeMichele & Sharpe, 1973; Buckley, 2019). The plants exhibiting such water-conserving behaviour are categorized as isohydric plants (Tardieu & Simonneau, 1998), and Taylaran *et al.* . (2011) reported that the root water uptake ability contributes to g_s through the leaf water status under steady-state conditions in rice. On the other hand, anisohydric plants allow for leaf water potential to decrease, maintaining higher g_s under drought conditions (Moshelion *et al.* , 2015). However, the relationship between the difference of isohydric and anisohydric strategies and photosynthetic induction remains unclear.

In this study, we used the rice genotypes ARC 11094 and Takanari, which exhibit rapid photosynthetic induction, and Koshihikari, which demonstrates slow photosynthetic induction. Koshihikari is one of the most popular rice cultivars in Japan. Takanari is a high-yielding cultivar in Japan and exhibits high photosynthetic activity in steady and non-steady states (Kanemura *et al.* , 2007; Takai *et al.* , 2013; Adachi *et al.* , 2019; Taniyoshi *et al.* , 2020). ARC 11094 is one of the genotypes belonging to the world rice core collection archived at the Genebank of the National Institute of Agrobiological Sciences (Kojima *et al.* , 2005), and showed the most rapid photosynthetic induction among 59 rice genotypes (Taniyoshi *et al.* , 2020). ARC 11094 showed high g_s at the initial phase during photosynthetic induction, and the dynamics was distinct from those of other rice genotypes (Taniyoshi *et al.* , 2020). Considering the relationship between stomatal dynamics and water status (Kaiser *et al.* , 2017; Sakoda *et al.* , 2021), it was hypothesized that with water use, the stomatal characteristics of ARC 11094 were different from those of Takanari and Koshihikari but similar to those of anisohydric plants. In this study, we evaluated photosynthetic induction, stomatal morphology, and water relations in plants as factors related to the CO_2 supply. In addition, the maximum rates of RuBP carboxylation, electron transport, and biochemical characteristics of the leaves were measured as factors related to CO_2 fixation. We also examined diurnal changes in the gas exchange rate in a field-mimicked environment. We aimed to uncover the detailed mechanisms underlying rapid photosynthetic induction and the relationship between water use strategy and photosynthetic induction in rice (*O. sativa* L.) through these analyses.

Materials and Methods

Plant cultivation

The seeds of ARC 11094 (ssp. indica), Takanari (ssp. indica) and Koshihikari (ssp. temperate japonica) were sown in nursery boxes filled with artificial soil on 19 April 2019, 21 April 2020 and 27 April 2021. The seedlings were transplanted to 2 L plastic pots filled with paddy soil (alluvial loam) at 28, 24, and 23 days after sowing in 2019, 2020, and 2021, respectively. Plants were grown at an experimental field site at the Graduate School of Agriculture, Kyoto University, Japan (35°2' N, 135°47' E, 65 m altitude). Slow-release fertilisers (ECOLONG413-100, JCAM AGRI. CO., Tokyo, Japan; volume and composition: 0.25 g N, 0.19 g P_2O_5 and 0.23 g K_2O) were applied to each pot as basal fertilizer. Subsequently, more slow-release fertilisers (ECOLONG413-40, JCAM AGRI. CO., Tokyo, Japan; volume and composition: 0.16 g N, 0.13 g P_2O_5 and 0.15 g K_2O) were applied to each pot one week before measurements. The water level of the pots was maintained at approximately 3 cm above the soil surface. These plants were measured at approximately three

months after sowing. To investigate the photosynthetic characteristics under changing osmotic potential, the three genotypes were cultivated in a greenhouse with the LED light source in an experimental field site at the Graduate School of Agriculture, Kyoto University, Japan (35°2 ‘N, 135°47’ E, 65 m altitude). Plants were cultivated in 2 L plastic pots with paddy soil (alluvial loam) and were measured at 47–49 days after sowing. The basal fertiliser (0.16 g N, 0.13 g P₂O₅ and 0.15 g K₂O) and the additional fertiliser 0.05 g N were applied to each pot. The environment in the greenhouse was set at a photoperiod of 13 h, a PPFD of 800 μmol photons m⁻²s⁻¹, and an air temperature of 20/28°C day/night.

Gas exchange rate measurements

Gas exchange rates at steady and non-steady states in the uppermost fully expanded leaves were measured using LI-6800 (LI-COR Inc., Lincoln, NE). The photosynthetic photon flux density (PPFD), air temperature, reference CO₂ concentration (CO₂R), and relative humidity (RH) in the leaf chamber were set to 1500 μmol photons m⁻² s⁻¹ (90% of red light and 10% of blue light), 30°C, 400 μmol mol⁻¹ and 55–65%, respectively, for the gas exchange measurement at steady state. A , g_s , intercellular CO₂ concentration (C_i), normalised A to a C_i of 250 μmol mol⁻¹ (A^*), transpiration rate (T), and water use efficiency (WUE) were recorded. A^* and WUE were calculated as follows:

$$A^* = \frac{A}{C_i} \times 250(1)WUE = \frac{A}{T} WUE = \frac{A}{T} \quad (2)$$

The response of A to C_i under steady-state conditions was obtained under the aforementioned conditions except for CO₂R, which was increased to 100, 200, 300, 400, 600, and 800 μmol mol⁻¹. The A - C_i curves were analysed using the equations of Farquhar *et al.* (1980) with the “Plantecophys” package in R (bilinear fitting method; Duursma, 2015) to estimate the maximum rates of RuBP carboxylation (V_{Cmax}) and electron transport (J_{max}). The parameters were normalised to 25°C during the fitting process based on Bernacchi *et al.* (2001).

Dark-adapted leaves of the plants under overnight dark treatment were used for gas exchange measurements in a non-steady state. The PPFD was changed from 0 μmol photons m⁻² s⁻¹ to 50 μmol photons m⁻² s⁻¹ for 10 min and then 1500 μmol photons m⁻²s⁻¹ for 90 min (Fig. S1a). The ratio of red–blue LED light sources was kept at 90:10. The photosynthetic parameters were recorded every 10 s. A dynamic A - C_i curve analysis was conducted based on previous studies (Soleh *et al.*, 2016; Taylor & Long, 2017). At first, the leaves were adapted to the steady state at PPFD of 1500 μmol photons m⁻² s⁻¹, air temperature of 30°C, CO₂R of 400 μmol mol⁻¹, and RH of 55–65%. Subsequently, the cycle of 50 μmol photons m⁻² s⁻¹ for 30 min and 1500 μmol photons m⁻² s⁻¹ for 10 min was repeated at CO₂R values of 100, 200, 300, 400, 600, and 800 μmol mol⁻¹. As described above, we obtained the dynamics of V_{Cmax} and J_{max} from the A - C_i curves fitted to the data for every 10 s interval.

Diurnal changes in gas exchange rates in a field-mimicked environment were measured using a LI-6400 (LI-COR Inc., Lincoln, NE). Overnight dark-adapted leaves were clamped within the leaf chamber, and the PPFD and air temperature used in Ohkubo *et al.* (2020) (Fig. S1b) was replicated for 12 h. Photosynthetic parameters at a CO₂R of 400 μmol mol⁻¹ were recorded every 10 s.

Nitrogen, Rubisco and Chlorophyll content

The uppermost-expanded leaves were sampled at 7–8 a.m. to evaluate nitrogen, RuBP carboxylase/oxygenase (Rubisco), and chlorophyll contents. Quantification was performed as described by Sakoda *et al.* (2020a). To quantify leaf nitrogen, the leaves were dried at 80°C for more than 72 h, weighed, and coarsely ground. The nitrogen content was determined by Kjeldahl digestion followed by an indophenol assay. To quantify Rubisco and chlorophyll, a leaf tissue of 1.5 cm² was collected, which was frozen immediately with liquid nitrogen and then stored at -80degC until further use. The leaf tissue was homogenised using a cold mortar and pestle in an extraction buffer containing 50 mM 4-(2-hydroxyethyl)-1-piperazineethanesulfonic acid (HEPES)-KOH, 5 mM MgCl₂, 1 mM Na₂ethylenediaminetetraacetic acid (EDTA), 0.1% (w/v) polyvinyl pyrrolidone (PVPP), 0.05% (v/v) Triton X-100, 5% glycerol, 4 mM amino-n-caproic acid, 0.8 mM benzamidine-HCl, and 5 mM dithiothreitol (DTT) at pH 7.4 with a small amount of quartz sand. A 200 μL aliquot was

separated for chlorophyll quantification. The homogenate was then centrifuged at $14,500 \times g$ for 5 min at 4°C . The supernatant was then used for Rubisco quantification. The Rubisco content was quantified spectrophotometrically by formamide extraction of the bands corresponding to the large and small subunits of Rubisco separated by SDS-PAGE (Makino *et al.*, 1986) using bovine serum albumin as the standard protein. The chlorophyll content extracted using 80% acetone was quantified spectrophotometrically as described by Porra *et al.* (1989).

Stomatal traits

Replicas of the adaxial and abaxial leaf surfaces used for gas exchange measurements were prepared using Suzuki's Universal Method of Printing. These replicas were observed at 100-fold magnification using an optical microscope (CX31 and DP21; Olympus, Tokyo, Japan). Three microscopic images were obtained for each replica. The stomatal density and guard cell length for each leaf was the sum and average of both surfaces, respectively. Additionally, specific stomatal conductance was calculated by dividing g_s by stomatal density to evaluate the contribution of a single stoma to g_s , following Ohsumi *et al.* (2007).

Water relations in plant

The leaf water potential (LWP) under steady state was measured by the pressure chamber method using Model670 (PMS Instrument Co., Albany, OR). The leaves were adapted to high light intensity ($1500 \mu\text{mol photons m}^{-2} \text{s}^{-1}$) for sufficient time before measurement. Whole-plant hydraulic conductance (K_{plant}) was calculated using the following equation, based on Hirasawa (1991):

$$K_{plant} = -\frac{T_{steady}}{LWP} \quad K_{plant} = -\frac{T_{steady}}{LWP} \quad (3)$$

where T_{steady} indicates T measured under the steady state.

The exudation rate per plant (E), root and shoot dry weights, and root/shoot ratio were measured to evaluate root activity. We cut the shoots of plants placed in the dark or after 10 min of irradiation with a PPFD of $50 \mu\text{mol photons m}^{-2} \text{s}^{-1}$ using a razor blade at 15 cm above the soil surface. Exudates were collected in pre-weighed cotton covered with plastic bags to prevent water loss by evaporation. After collection for 30 min, the volume was calculated based on the difference in the weight of cotton. The exudate for measuring osmotic potential was also collected using a micropipette. The roots and shoots of the plants were washed with water carefully, and parts of the roots were separated to evaluate the root area. Separated root samples were scanned using a GT-S640 (SEIKO EPSON CO., Nagano, Japan) at a resolution of 800 dpi, and the projected root area was estimated using ImageJ software (National Institutes of Health, Bethesda, MD). All the samples were dried at 80°C for more than 72 h and then weighed. We calculated the normalised E to root or shoot dry weight ($E/Root$ and $E/Shoot$, respectively) to remove the effects of differences in individual growth. The osmotic potential of the exudate ($\Psi_{\xi\psi\lambda\epsilon\mu\sigma\alpha\pi}$) was measured using a freezing point osmometer (OM802, Vogel, Giessen, Germany), as described by Adachi *et al.* (2017). The root hydraulic conductance ($L_P(os)$) and conductivity ($L_{Pr}(os)$) were calculated using the following equations:

Hosted file

image2.emf available at <https://authorea.com/users/394570/articles/576492-anisohydric-characteristics-of-a-rice-genotype-arc-11094-contribute-to-increased-photosynthetic-carbon-fixation-under-fluctuating-light-conditions>

$$L_P(os) = \frac{E}{\sigma(\Psi_{soil\ os} - \Psi_{xylem\ sap})} \quad (4)$$

$$L_{Pr}(os) = \frac{L_P(os)}{\text{Root projected area}} \quad L_{Pr}(os) = \frac{L_P(os)}{\text{Whole root projected area}} \quad (5)$$

where $\Psi_{soil\ os}$ is the osmotic potential of the surface water in the pots. We used a value of 0.4 for σ and a value of -0.012 MPa for $\Psi_{soil\ os}$ following Miyamoto *et al.* (2001) and Adachi *et al.* (2017). The whole root projected area was estimated by whole root dry weight and the ratio of root-projected area to root dry weight in a separated root sample.

Photosynthetic response to changing osmotic potential

To characterise the photosynthetic response to leaf water deficit, we observed dynamics of g_s under varying osmotic potential. Leaves were cut below the collar, then immediately cut again when immersed in the water to avoid the cavitation, and arranged with water using 15 mL tubes. The leaves were clamped within the leaf chamber of LI-6800, which was set at a PPFD of 1500 $\mu\text{mol photons m}^{-2} \text{ s}^{-1}$, an air temperature of 30°C, a CO_2R concentration of 400 $\mu\text{mol mol}^{-1}$, and a RH of 55-65%. After stabilization of photosynthesis, 1% (w/v) PEG-4000 was added until the final concentration of the PEG-4000 to 0.1% (w/v) is achieved and the solution was stirred gently. Photosynthetic parameters were recorded every 10 s when the osmotic potential changed.

Statistical analysis

The values of all parameters were averaged for the specific genotype or treatment, and the standard error was calculated. The Tukey–Kramer multiple comparison test was used to compare the means. All analyses were performed using Microsoft Excel (Microsoft, Redmond, WA) and the R software (R Foundation for Statistical Computing, Vienna, Austria).

Results

Gas exchange rate at steady and non-steady state

First, the photosynthetic parameters under steady state (A_{steady} , $g_{s,steady}$, $C_{i,steady}$, A^*_{steady} , T_{steady} , WUE_{steady}) were measured. A_{steady} values for ARC 11094, Takanari, and Koshihikari were 26.1, 29.2, 22.5 $\mu\text{mol CO}_2\text{m}^{-2} \text{ s}^{-1}$, respectively (Table 1). ARC 11094 and Takanari showed greater $g_{s,steady}$ than Koshihikari, but $C_{i,steady}$ of Takanari was similar to that of Koshihikari (Table 1). Therefore, the A^*_{steady} of Takanari tended to be greater than that of ARC 11094 and Koshihikari (Table 1). The T_{steady} of ARC 11094 and Takanari was higher than that of Koshihikari, and ARC 11094 showed lower WUE_{steady} than those of Takanari and Koshihikari because of the lower A^*_{steady} (Table 1).

Next, we investigated the response of the photosynthetic parameters to fluctuating light conditions. After step increases in light intensity, A of ARC 11094 and Takanari increased more rapidly than that of Koshihikari, where the time to reach 80% of the maximum A during induction response ($T_{80,A}$) in ARC 11094, Takanari, and Koshihikari were 13.9, 16.2 and 37.0 minutes, respectively (Fig. 1a,g; Table S1). However, the values of A in the dark (R_d) and just before high light irradiation ($A_{initial}$), and the maximum values during induction (A_{max}), and the time to reach 50% of the maximum A during induction response ($T_{50,A}$) were not significantly different among all the genotypes (Table S1). A^* in the dark and before high light irradiation (A^*_{dark} , $A^*_{initial}$), the maximum values of g_s and A^* during induction response ($g_{s,max}$, A^*_{max}), and the time to reach 50% of $g_{s,max}$ and A^*_{max} (T_{50,g_s} and T_{50,A^*}) also showed no significant differences. The g_s in dark ($g_{s,dark}$), and the time to reach 80% of $g_{s,max}$ and A^*_{max} (T_{80,g_s} and T_{80,A^*}) were higher or shorter in ARC 11094 and Takanari than Koshihikari (Fig. 1b,d,h,i; Table S1). In ARC 11094 and Takanari, g_s prior to high light irradiation ($g_{s,initial}$) tended to be higher than that in Koshihikari ($P = 0.057$; Table S1). The values of g_s , A^* , and T in ARC 11094 and Takanari increased more rapidly and were higher than those in Koshihikari (Fig. 1b,d,e). C_i was also higher in ARC 11094 and Takanari than in Koshihikari (Fig. 1c). In contrast, the WUE of Koshihikari was higher than that of ARC 11094 and Takanari during the induction response (Fig. 1f). Similar results were obtained in plants grown in a greenhouse with the LED light source (Fig. S2).

Diurnal changes of gas exchange rate under field mimicked environment

PPFD in the rice canopy fluctuated drastically and affected all photosynthetic parameters (Fig. 2, S1b). ARC 11094 had greater A , g_s , A^* , and T values than Koshihikari throughout the day (Fig. 2a,b,d,e). Takanari had higher A , g_s and T than Koshihikari during most of the day, but slightly lower than Koshihikari in the late afternoon (Fig. 2a,b,e). C_i of Takanari tended to be higher, and the WUE of ARC 11094 and Takanari tended to be lower than that of Koshihikari in the morning (Fig. 2c,f).

Dynamic $A-C_i$ curve analysis

As CO_2R increased, A became higher, and the slope of the $A-C_i$ curves increased with time in all genotypes (Fig. 3). In ARC 11094 and Takanari, the A responses were more rapid under each CO_2R , and the slope of the $A-C_i$ curves was steeper than in Koshihikari (Fig. 3). V_{Cmax} and J_{max} increased during the induction response for all genotypes (Fig. 4). The V_{Cmax} of all genotypes was not different in the initial induction phase. Still, ARC 11094 and Takanari showed slightly higher values than Koshihikari 4 min after a step increase in light intensity (Fig. 4a). J_{max} of ARC 11094 and Takanari was also high, and that of Koshihikari was low during the induction response (Fig. 4b). Considering the steady state values as 100%, relative V_{Cmax} and J_{max} in Takanari were similar to or lower than that of Koshihikari (Fig. S3). ARC 11094 showed higher relative V_{Cmax} and J_{max} than Takanari and Koshihikari (Fig. S3).

Biochemical traits related to leaf photosynthesis

Nitrogen, Rubisco, and chlorophyll contents were investigated as traits related to CO_2 fixation. The nitrogen content per leaf area of ARC 11094 was significantly lower than that of Takanari and Koshihikari (Fig. S4a). There were no significant differences among the genotypes in the nitrogen content per leaf dry weight, Rubisco content per leaf area and per leaf dry weight, and chlorophyll content per leaf area (Fig. S4b,c,d,e). However, the chlorophyll content per leaf dry weight was higher in ARC 11094 than in Takanari and Koshihikari (Fig. S4f).

Stomatal traits and water relations

ARC 11094 and Koshihikari had similar stomatal densities, and Takanari had higher values than the other two genotypes (Fig. 5a). On the other hand, the guard cell length of Takanari was the lowest, followed in order by Koshihikari and ARC 11094 (Fig. 5b). To estimate the contribution of a single stoma to g_s , we calculated specific g_s . Specific g_s values of ARC 11094 were higher in Takanari and Koshihikari, and Takanari showed similar values to Koshihikari after 40 min of irradiation (Fig. 5c).

The LWP and K_{plant} under saturating light tended to be lower in ARC 11094 than in Takanari and Koshihikari (Table 1). Exudation rate per plant (E) and normalised E to root and shoot dry weight ($E/Root$ and $E/Shoot$) were measured under dark or low light for 10 min as an indicator of water transport from root to shoot. There was no apparent difference between the two light treatments in any genotype (Fig. 6a,b,c). The E of Takanari was significantly higher than that of ARC 11094 and Koshihikari (Fig. 6a). The $E/Root$ of ARC 11094 was lower than that of Takanari and Koshihikari, and Takanari and Koshihikari showed similar $E/Root$ (Fig. 6b). However, $E/Shoot$ of ARC 11094 was higher than that of Koshihikari under dark conditions (Fig. 6c). Although the root dry weights of ARC 11094 and Takanari were significantly higher than those of Koshihikari ($p < 0.05$), the shoot dry weight of ARC 11094 was lower than those of Takanari and Koshihikari, resulting in a remarkably higher root/shoot ratio in ARC 11094 (Fig. 6d,e,f). We also evaluated the root hydraulic conductance (L_P (os)) based on E and the osmotic potential of exudate ($\Psi_{\xi\psi\lambda\epsilon\mu\sigma\pi}$). We then calculated the root hydraulic conductivity (L_{Pr} (os)) by dividing L_P (os) by the whole root projected area. Significant varietal differences were observed only in L_P (os) under the dark and whole-root projected areas (Fig. S5).

A , g_s , C_i and T of all genotypes showed a significant decrease approximately 5 min after changing the osmotic potential (Fig. 7a,b,c,e). However, the parameters of ARC 11094 recovered slightly and maintained higher values compared to the other two genotypes 10 min after the initial treatment (Fig. 7a,b,c,e). On the other hand, WUE of all genotypes increased approximately 5 min after changing the osmotic potential (Fig. 7f). However, the increase of WUE in ARC 11094 was less than those in Takanari and Koshihikari (Fig. 7f). A^* did not show apparent differences among genotypes (Fig. 7d).

Discussion

ARC 11094 and Takanari genotypes showed a more rapid photosynthetic induction than Koshihikari did. This result is attributable to the apparent mesophyll cell activity and CO_2 diffusion from the atmosphere into the leaves, as shown by the dynamics of A^* , V_{Cmax} , J_{max} , and g_s (Fig. 1, 4, S2; Table S1). However, there

were no apparent differences in the relative values of V_{Cmax} and J_{max} between the Takanari and Koshihikari plants during the induction response (Fig. S3). Efficient CO₂ fixation in ARC 11094 (Fig. 1, 4, S2, S3; Table S1) may be related to the nitrogen distribution or chlorophyll content per leaf dry weight (Fig. S4a,f); however, a detailed study is required to determine the specific factor. ARC 11094 and Takanari showed higher A^* values and maintained a higher C_i than Koshihikari during the induction response (Fig. 1, S2; Table S1). Taken together, both CO₂ fixation and supply are essential for rapid photosynthetic induction, but CO₂ supply may be more dominant than CO₂ fixation to limit non-steady-state photosynthesis in ARC 11094, Takanari, and Koshihikari. These results are consistent with those of De Souza *et al.* (2020), Eyland *et al.* (2021) and Zhang *et al.* (2022).

Previous reports have shown that stomatal conductance immediately before high light irradiation is essential for subsequent photosynthetic induction (Soleh *et al.*, 2017; Wachendorf & Küppers, 2017a,b; Taniyoshi *et al.*, 2020). In the present study, ARC 11094 and Takanari showed significantly greater $g_{s, dark}$ than Koshihikari. The varietal order was consistent in $g_{s, initial}$, although it was not statistically significant ($p = 0.057$) (Fig. 1b; Table S1). Therefore, the greater g_s during the induction response is attributable to greater $g_{s, dark}$ and sensitivity to low light in ARC 11094 and Takanari. The *slow anion channel-associated 1 (SLAC1)* or *open stomata 1 (OST1)* contributes to stomatal closure in response to abscisic acid and high CO₂ (Xue *et al.*, 2011), and these deficient mutants show higher $g_{s, dark}$ than wild-type plants in *Arabidopsis* (Kimura *et al.*, 2020). Therefore, abscisic acid or high CO₂ sensitivity may be related to the high $g_{s, dark}$ in ARC 11094 and Takanari. In addition, the stomatal response induced by blue light occurs and is saturated under low light intensity (<5-10 $\mu\text{mol photons m}^{-2} \text{ s}^{-1}$; Shimazaki *et al.*, 2007; Matthews *et al.*, 2020). Thus, stomatal opening in response to low light in ARC 11094 and Takanari may be related to the blue light response of the stomata.

The stomatal morphology was distinct among the three genotypes (Fig. 5a,b). Takanari had a higher stomatal density and smaller stomatal size than ARC 11094 and Koshihikari (Fig. 5a,b). These characteristics have been reported to be advantageous for the response of stomatal conductance to fluctuating light (Faralli *et al.*, 2019; Zhang *et al.*, 2019; Lawson & Matthews, 2020; Sakoda *et al.*, 2020b; Xiong *et al.*, 2022). The stomatal morphology of ARC 11094 was similar to that of Koshihikari (Fig. 5a,b). Therefore, the contribution of a single stoma to stomatal conductance, such as stomatal aperture or pore depth, was significant in ARC 11094 compared to Takanari and Koshihikari (Fig. 5c). Altogether, high stomatal conductance during the induction response is related to stomatal morphology in Takanari and single stomatal behaviour in ARC 11094.

Root water uptake ability can affect leaf photosynthesis through leaf water potential and stomatal conductance (Hirasawa, 1991; Taylaran *et al.*, 2011). The E of Takanari was superior to those of ARC 11094 and Koshihikari under dark and low light conditions, which was attributable to the greater root mass (Fig. 6). These results are consistent with those of Taylaran *et al.* (2011) and imply that root water uptake ability contributes to the rapid response of stomatal conductance to a step increase in light intensity in Takanari. In ARC 11094, the root mass was similar to that in Takanari, resulting in the highest root/shoot ratio (Fig. 6d,e). However, K_{plant} under high light intensity and $E/Root$ under dark or low light conditions were lower in ARC 11094 than that in Takanari and Koshihikari (Table 1; Fig. 6b). ARC 11094 could not utilise the large root mass efficiently, as similar results can be seen in $L_P (os)$ or $L_{Pr} (os)$ (Fig. S5b,d). Therefore, the water supply from roots to leaves was insufficient against large g_s , and the LWP under saturating light was low in ARC 11094 (Table 1).

Why can ARC 11094 realise the great g_s under the non-steady state even though the root water uptake ability is low? In general, leaf water deficit induces hydroactive stomatal closure (Glinka, 1971; DeMichele & Sharpe, 1973; Buckley, 2019). Koshihikari showed temporary setback of g_s during photosynthetic induction, which would be attributable to hydroactive stomatal closure (Fig. 1b, S2b). However, Takanari did not demonstrate such a setback because of the large water uptake ability (Fig. 1b, 6, S2b, S5). This stomatal behavior of Koshihikari and Takanari resemble the characteristics in isohydric plants (Tardieu & Simonneau, 1998; Moshelion *et al.*, 2015). In contrast to Koshihikari and Takanari, ARC 11094 maintained higher g_s

after changing the osmotic potential (Fig. 7b). This result indicates stomata of ARC 11094 is unsusceptible to low leaf water potential, and has similar characteristics to those of anisohydric plants. Altogether, ARC 11094 may realise the rapid response of g_s to fluctuating light because of the anisohydric stomatal behaviour, which is consistent with the lower WUE under field-mimicked environments (Fig. 2). These characteristics may contribute to the rapid photosynthetic induction and significant carbon gain under fluctuating light conditions; however, the total dry weight was lowest in ARC 11094 (Fig. 2a, 6e,f). The low biomass production in ARC 11094 is probably due to the adverse effects of drought stress induced by the unique water management system that reduced the benefits of rapid photosynthetic induction. Similar phenomena have been observed in previous studies using *slac1* deficit rice or *STOMAGEN*-overexpressing *Arabidopsis* (Tanaka *et al.* , 2013; Sakoda *et al.* , 2020b; Yamori *et al.* , 2020). However, anisohydric plants are reported to exhibit high biomass production under ample water supply in *Populus* genus (Attia *et al.* , 2015). These results suggest that optimising the water balance at the whole-plant level, depending on the environments or objectives, is important for enhancing biomass production by utilising the photosynthetic induction response. Isohydric and anisohydric stomatal behaviors are thought to be related to abscisic acid biosynthesis or aquaporin expression (Galle *et al.* , 2013; Moshelion *et al.* , 2015; Shelden *et al.* , 2017); however, the detailed mechanism remains unclear. If the genetic factors and molecular mechanisms for the rapid photosynthetic induction of ARC 11094 are elucidated, a suitable approach to improve stomatal characteristics can be devised.

The present study characterised the underlying factors on natural variation of photosynthetic induction response using three rice genotypes. ARC 11094 and Takanari showed higher CO_2 supply during the induction response than Koshihikari. The CO_2 supply in Takanari is related to stomatal density, size, and root mass. The CO_2 supply of ARC 11094 is related to stomatal aperture or pore depth. Additionally, ARC 11094 showed the anisohydric stomatal behaviour and maintained stomatal opening under water-insufficient conditions in leaves. As shown in the present study, there are various strategies for rapid photosynthetic induction, and ARC 11094 has the unique mechanism for stomatal response to fluctuating light environments in terms of water relations. Stomatal manipulation has been attempted to improve the CO_2 supply during the induction response (Papanatsiou *et al.* , 2019; Kimura *et al.* , 2020; Sakoda *et al.* , 2020b; Yamori *et al.* , 2020). However, the regulation of stomatal traits and water balance at the whole-plant level should focus on long-term adaptation to abiotic stress and biomass production in field environments. Understanding and combining these characteristics could lead to further rapid photosynthetic induction and improve crop productivity in field environments.

Acknowledgement

This work was supported in part by a Sasakawa Scientific Research Grant from the Japan Science Society (grant no. 2020-4014 to K.T.), the Japan Science and Technology Agency, PRESTO (grant no. JP-MJPR16Q5 to Y.T.), and JSPS KAKENHI (grant no. 20H02968 to Y.T, 19H02939, and 21K19104 to S.A. and Y.T.).

Author Contributions

K.T., Y.T., and T.S. designed the experiments; K.T. conducted most of the measurements and S.A. measured the osmotic potential of the exudate; K.T., Y.T., and S.A. prepared and finalised the manuscript.

Data Availability

The data supporting the findings of this study are available from the corresponding author upon reasonable request.

References

- Acevedo-Siaca LG, Coe R, Quick WP, Long SP. 2021. Variation between rice accessions in photosynthetic induction in flag leaves and underlying mechanisms. *Journal of Experimental Botany* **72** : 1282–1294.
- Acevedo-Siaca LG, Coe R, Wang Y, Kromdijk J, Quick WP, Long SP. 2020. Variation in photo-

synthetic induction between rice accessions and its potential for improving productivity. *New Phytologist* **227** : 1097–1108.

Adachi S, Ookawa T, Hirasawa T. 2017. A quick determination of root resistance to water transport in paddy rice. *Plant Production Science* **20** : 273–278.

Adachi S, Tanaka Y, Miyagi A, Kashima M, Tezuka A, Toya Y, Kobayashi S, Ohkubo S, Shimizu H, Kawai-Yamada M et al. 2019. High-yielding rice Takanari has superior photosynthetic response to a commercial rice Koshihikari under fluctuating light. *Journal of Experimental Botany* **70** : 5287–5297.

Attia Z, Domec JC, Oren R, Way DA, Moshelion M. 2015. Growth and physiological responses of isohydric and anisohydric poplars to drought. *Journal of Experimental Botany* **66** : 4373–4381.

Bernacchi CJ, Singaas EL, Pimentel C, Portis AR, Long SP. 2001. Improved temperature response functions for models of Rubisco-limited photosynthesis. *Plant, Cell & Environment* **24** : 253–259.

Buckley TN. 2019. How do stomata respond to water status? *New Phytologist* **224** : 21–36.

DeMichele DW, Sharpe PJH. 1973. An analysis of the mechanics of guard cell motion. *Journal of Theoretical Biology* **41** : 77–96.

De Souza AP, Wang Y, Orr DJ, Carmo-Silva E, Long SP. 2020. Photosynthesis across African cassava germplasm is limited by Rubisco and mesophyll conductance at steady state, but by stomatal conductance in fluctuating light. *New Phytologist* **225** : 2498–2512.

Duursma RA. 2015. Plantecophys - An R package for analysing and modelling leaf gas exchange data. *PLOS ONE* **10** : e0143346.

Eyland D, van Wesemael J, Lawson T, Carpentier S. 2021. The impact of slow stomatal kinetics on photosynthesis and water use efficiency under fluctuating light. *Plant Physiology* **186** : 998–1012.

Faralli M, Matthews J, Lawson T. 2019. Exploiting natural variation and genetic manipulation of stomatal conductance for crop improvement. *Current Opinion in Plant Biology* **49** : 1–7.

Farquhar GD, von Caemmerer S, Berry JA. 1980. A biochemical model of photosynthetic CO₂ assimilation in leaves of C₃ species. *Planta* **149** : 78–90.

Gallé Á, Csizsár J, Benyó D, Laskay G, Leviczky T, Erdei L, Tari I. 2013. Isohydric and anisohydric strategies of wheat genotypes under osmotic stress: Biosynthesis and function of ABA in stress responses. *Journal of Plant Physiology* **170** : 1389–1399.

Glinka Z. 1971. The effect of epidermal cell water potential on stomatal response to illumination of leaf discs of *Vicia faba*. *Physiologia Plantarum* **24** : 476–479.

Harrison EL, Cubas LA, Gray JE, Hepworth C. 2020. The influence of stomatal morphology and distribution on photosynthetic gas exchange. *Plant Journal: For Cell and Molecular Biology* **101** : 768–779.

Hirasawa T, Ishihara K. 1991. On resistance to water transport in crop plants for estimating water uptake ability under intense transpiration. *Japanese Journal of Crop Science* **60** : 174–183.

Hirasawa T, Tsuchida M, Ishihara K. 1992. Relationship between resistance to water transport and exudation rate and the effect of the resistance on the midday depression of stomatal aperture in rice plants. *Japanese Journal of Crop Science* **61** : 145–152.

Kaiser E, Morales A, Harbinson J, Heuvelink E, Prinzenberg AE, Marcelis LFM. 2016. Metabolic and diffusional limitations of photosynthesis in fluctuating irradiance in *Arabidopsis thaliana*. *Scientific Reports* **6** : 31252.

Kaiser E, Kromdijk J, Harbinson J, Heuvelink E, Marcelis LFM. 2017. Photosynthetic induction and its diffusional, carboxylation and electron transport processes as affected by CO₂ partial pressure, temperature, air humidity and blue irradiance. *Annals of Botany* **119** : 191–205.

Kanemura T, Homma K, Ohsumi A, Shiraiwa T, Horie T. 2007. Evaluation of genotypic variation in leaf photosynthetic rate and its associated factors by using rice diversity research set of germplasm. *Photosynthesis Research* **94** : 23–30.

Kimura H, Hashimoto-Sugimoto M, Iba K, Terashima I, Yamori W. 2020. Improved stomatal opening enhances photosynthetic rate and biomass production in fluctuating light. *Journal of Experimental Botany* **71** : 2339–2350.

Kojima Y, Ebana K, Fukuoka S, Nagamine T, Kawase M. 2005. Development of an RFLP-based rice diversity research set of germplasm. *Breeding Science* **55** : 431–440.

Kromdijk J, Głowacka K, Leonelli L, Gabilly ST, Iwai M, Niyogi KK, Long SP. 2016. Improving photosynthesis and crop productivity by accelerating recovery from photoprotection. *Science* **354** : 857–861.

Lawson T, Matthews J. 2020. Guard cell metabolism and stomatal function. *Annual Review of Plant Biology* **71** : 273–302.

Long SP, Zhu XG, Naidu SL, Ort DR. 2006. Can improvement in photosynthesis increase crop yields? *Plant, Cell & Environment* **29** : 315–330.

López-Calcano PE, Brown KL, Simkin AJ, Fisk SJ, Vialet-Chabrand S, Lawson T, Raines CA. 2020. Stimulating photosynthetic processes increases productivity and water-use efficiency in the field. *Nature Plants* **6** : 1054–1063.

Makino A, Mae T, Ohira K. 1986. Colorimetric measurement of protein stained with coomassie brilliant blue r on sodium dodecyl sulfate-polyacrylamide gel electrophoresis by eluting with formamide. *Agricultural and Biological Chemistry* **50** : 1911–1912.

Matthews JSA, Vialet-Chabrand S, Lawson T. 2020. Role of blue and red light in stomatal dynamic behaviour. *Journal of Experimental Botany* **71** : 2253–2269.

McAusland L, Vialet-Chabrand S, Davey P, Baker NR, Brendel O, Lawson T. 2016. Effects of kinetics of light-induced stomatal responses on photosynthesis and water-use efficiency. *New Phytologist* **211** : 1209–1220.

Miyamoto N, Steudle E, Hirasawa T, Lafitte R. 2001. Hydraulic conductivity of rice roots. *Journal of Experimental Botany* **52** : 1835–1846.

Moshelion M, Halperin O, Wallach R, Oren R, Way DA. 2015. Role of aquaporins in determining transpiration and photosynthesis in water-stressed plants: crop water-use efficiency, growth and yield. *Plant, Cell & Environment* **38** : 1785–1793.

Ohkubo S, Tanaka Y, Yamori W, Adachi S. 2020. Rice cultivar Takanari has higher photosynthetic performance under fluctuating light than Koshihikari, especially under limited nitrogen supply and elevated CO₂. *Frontiers in Plant Science* **11** : 1308.

Ohsumi A, Kanemura T, Homma K, Horie T, Shiraiwa T. 2007. Genotypic variation of stomatal conductance in relation to stomatal density and length in rice (*Oryza sativa* L.). *Plant Production Science* **10** : 322–328.

Papanatsiou M, Petersen J, Henderson L, Wang Y, Christie JM, Blatt MR. 2019. Optogenetic manipulation of stomatal kinetics improves carbon assimilation, water use, and growth. *Science* **363** : 1456–1459.

Pearcy RW. 1990. Sunflecks and photosynthesis in plant canopies. *Annual Review of Plant Physiology and Plant Molecular Biology* **41** : 421–453.

Pearcy RW, Way DA. 2012. Two decades of sunfleck research: looking back to move forward. *Tree Physiology* **32** : 1059–1061.

Porra RJ, Thompson WA, Kriedemann PE. 1989. Determination of accurate extinction coefficients and simultaneous equations for assaying chlorophylls a and b extracted with four different solvents: verification of the concentration of chlorophyll standards by atomic absorption spectroscopy. *Biochimica et Biophysica Acta* **975** : 384–394.

Qu M, Hamdani S, Li W, Wang S, Tang J, Chen Z, Song Q, Li M, Zhao H, Chang T et al. 2016. Rapid stomatal response to fluctuating light: An under-explored mechanism to improve drought tolerance in rice. *Functional Plant Biology: FPB* **43** : 727–738.

Sakoda K, Kaga A, Tanaka Y, Suzuki S, Fujii K, Ishimoto M, Shiraiwa T. 2020a. Two novel quantitative trait loci affecting the variation in leaf photosynthetic capacity among soybeans. *Plant Science* **291** : 110300.

Sakoda K, Yamori W, Shimada T, Sugano SS, Hara-Nishimura I, Tanaka Y. 2020b. Higher stomatal density improves photosynthetic induction and biomass production in *Arabidopsis* under fluctuating light. *Frontiers in Plant Science* **11** : 589603.

Sakoda K, Taniyoshi K, Yamori W, Tanaka Y. 2022. Drought stress reduces crop carbon gain due to delayed photosynthetic induction under fluctuating light conditions. *Physiologia Plantarum* **174** : e13603.

Salter WT, Li S, Dracatos PM, Barbour MM. 2020. Identification of quantitative trait loci for dynamic and steady-state photosynthetic traits in a barley mapping population. *AoB Plants*. doi: 10.1093/aob-pla/plaa063.

Salter WT, Merchant AM, Richards RA, Trethowan R, Buckley TN. 2019. Rate of photosynthetic induction in fluctuating light varies widely among genotypes of wheat. *Journal of Experimental Botany* **70** : 2787–2796.

Shelden MC, Vandeleur R, Kaiser BN, Tyerman SD. 2017. A comparison of petiole hydraulics and aquaporin expression in an anisohydric and isohydric cultivar of grapevine in response to water-stress induced cavitation. *Frontiers in Plant Science* **8** : 1893.

Shimazaki KI, Doi M, Assmann SM, Kinoshita T. 2007. Light regulation of stomatal movement. *Annual Review of Plant Biology* **58** : 219–247.

Slattery RA, Walker BJ, Weber APM, Ort DR. 2018. The impacts of fluctuating light on crop performance. *Plant Physiology* **176** : 990–1003.

Soleh MA, Tanaka Y, Kim SY, Huber SC, Sakoda K, Shiraiwa T. 2017. Identification of large variation in the photosynthetic induction response among 37 soybean [*Glycine max* (L.) Merr.] genotypes that is not correlated with steady-state photosynthetic capacity. *Photosynthesis Research* **131** : 305–315.

Soleh MA, Tanaka Y, Nomoto Y, Iwahashi Y, Nakashima K, Fukuda Y, Long SP, Shiraiwa T. 2016. Factors underlying genotypic differences in the induction of photosynthesis in soybean [*Glycine max* (L.) Merr.]. *Plant Cell and Environment* **39** : 685–693.

Takai T, Adachi S, Taguchi-Shiobara F, Sanoh-Arai Y, Iwasawa N, Yoshinaga S, Hirose S, Taniguchi Y, Yamanouchi U, Wu J et al. 2013. A natural variant of *NAL1*, selected in high-yield rice breeding programs, pleiotropically increases photosynthesis rate. *Scientific Reports* **3** : 2149.

Tanaka Y, Sugano SS, Shimada T, Hara-Nishimura I. 2013. Enhancement of leaf photosynthetic capacity through increased stomatal density in *Arabidopsis*. *New Phytologist* **198** : 757–764.

Tanaka Y, Adachi S, Yamori W. 2019. Natural genetic variation of the photosynthetic induction response to fluctuating light environment. *Current Opinion in Plant Biology* **49** : 52–59.

Taniyoshi K, Tanaka Y, Shiraiwa T. 2020. Genetic variation in the photosynthetic induction response in rice (*Oryza sativa* L.). *Plant Production Science* **23** : 513–521.

Tardieu F, Simonneau T. 1998. Variability among species of stomatal control under fluctuating soil water status and evaporative demand: modelling isohydric and anisohydric behaviours. *Journal of Experimental Botany* **49** : 419–432.

Taylaran RD, Adachi S, Ookawa T, Usuda H, Hirasawa T. 2011. Hydraulic conductance as well as nitrogen accumulation plays a role in the higher rate of leaf photosynthesis of the most productive variety of rice in Japan. *Journal of Experimental Botany* **62** : 4067–4077.

Taylor SH, Long SP. 2017. Slow induction of photosynthesis on shade to sun transitions in wheat may cost at least 21% of productivity. *Philosophical Transactions of the Royal Society of London. Series B, Biological Sciences* **372** : 20160543.

Wachendorf M, Küppers M. 2017a. Effects of leaf temperature on initial stomatal opening and their roles in overall and biochemical photosynthetic induction. *Trees* **31** : 1667–1681.

Wachendorf M, Küppers M. 2017b. The effect of initial stomatal opening on the dynamics of biochemical and overall photosynthetic induction. *Trees* **31** : 981–995.

Xiong Z, Dun Z, Wang Y, Yang D, Xiong D, Cui K, Peng S, Huang J. 2022. Effect of stomatal morphology on leaf photosynthetic induction under fluctuating light in rice. *Frontiers in Plant Science* **12** : 754790.

Xue S, Hu H, Ries A, Merilo E, Kollist H, Schroeder JI. 2011. Central functions of bicarbonate in S-type anion channel activation and OST1 protein kinase in CO₂ signal transduction in guard cell. *The EMBO Journal* **30** : 1645–1658.

Yamori W. 2016. Photosynthetic response to fluctuating environments and photoprotective strategies under abiotic stress. *Journal of Plant Research* **129** : 379–395.

Yamori W, Kusumi K, Iba K, Terashima I. 2020. Increased stomatal conductance induces rapid changes to photosynthetic rate in response to naturally fluctuating light conditions in rice. *Plant Cell and Environment* **43** : 1230–1240.

Yamori W, Makino A, Shikanai T. 2016. A physiological role of cyclic electron transport around photosystem I in sustaining photosynthesis under fluctuating light in rice. *Scientific Reports* **6** : 20147.

Yamori W, Masumoto C, Fukayama H, Makino A. 2012. Rubisco activase is a key regulator of non-steady-state photosynthesis at any leaf temperature and, to a lesser extent, of steady-state photosynthesis at high temperature. *Plant Journal: For Cell and Molecular Biology* **71** : 871–880.

Zhang N, Berman SR, Joubert D, Violet-Chabrand S, Marcelis LFM, Kaiser E. 2022. Variation of photosynthetic induction in major horticultural crops is mostly driven by differences in stomatal traits. *Frontiers in Plant Science* **13** : 860229.

Zhang Q, Peng S, Li Y, Lawson T. 2019. Increase rate of light-induced stomatal conductance is related to stomatal size in the genus *Oryza*. *Journal of Experimental Botany* **70** : 5259–5269.

Zhu X-G, Long SP, Ort DR. 2010. Improving photosynthetic efficiency for greater yield. *Annual Review of Plant Biology* **61** : 235–261.

Table 1 Photosynthetic parameters and water relations in plants under steady-state. CO₂ assimilation rate (A_{steady}), stomatal conductance ($g_{s,steady}$), intercellular CO₂ concentration ($C_{i,steady}$), normalized CO₂ assimilation rate to a C_i of 250 $\mu\text{mol mol}^{-1}$ (A^*_{steady}), transpiration rate (T_{steady}) and water use

efficiency (WUE_{steady}) were measured with LI-6800 at a PPFD of 1500 $\mu\text{mol photons m}^{-2} \text{s}^{-1}$, a reference CO_2 concentration of 400 $\mu\text{mol mol}^{-1}$, an air temperature of 30°C and a relative humidity of 55–65%. Leaf water potential (LWP) was evaluated immediately after the photosynthetic measurement with the pressure chamber method. Whole plant hydraulic conductance (K_{plant}) was calculated using the values of T_{steady} and LWP . Values are mean \pm SE ($n = 4$). Lower-case letters represent significant differences among genotypes at $P < 0.05$ (Tukey–Kramer multiple comparison test).

Parameters	ARC 11094	Takanari	Koshihikari
A_{steady} ($\mu\text{mol CO}_2 \text{ m}^{-2} \text{ s}^{-1}$)	26.1 \pm 1.3	ab 29.2 \pm 1.8	a 22.5 \pm 1.9
$g_{s,steady}$ ($\text{mol H}_2\text{O m}^{-2} \text{ s}^{-1}$)	0.51 \pm 0.03	a 0.47 \pm 0.04	a 0.33 \pm 0.03
$C_{i,steady}$ ($\mu\text{mol CO}_2 \text{ mol}^{-1}$)	287 \pm 3	a 263 \pm 4	b 258 \pm 2
A^*_{steady} ($\mu\text{mol CO}_2 \text{ m}^{-2} \text{ s}^{-1}$)	22.8 \pm 1.3	27.8 \pm 1.8	21.8 \pm 1.8
T_{steady} ($\text{mmol H}_2\text{O m}^{-2} \text{ s}^{-1}$)	7.1 \pm 0.2	a 6.7 \pm 0.4	a 5.3 \pm 0.4
WUE_{steady} ($\mu\text{mol CO}_2 \text{ mmol}^{-1} \text{ H}_2\text{O}$)	3.7 \pm 0.1	b 4.4 \pm 0.1	a 4.3 \pm 0.1
LWP (MPa)	-0.60 \pm 0.12	-0.40 \pm 0.06	-0.33 \pm 0.04
K_{plant} ($\text{mmol H}_2\text{O m}^{-2} \text{ s}^{-1} \text{ MPa}^{-1}$)	13.2 \pm 2.5	17.6 \pm 3.6	17.7 \pm 1.5

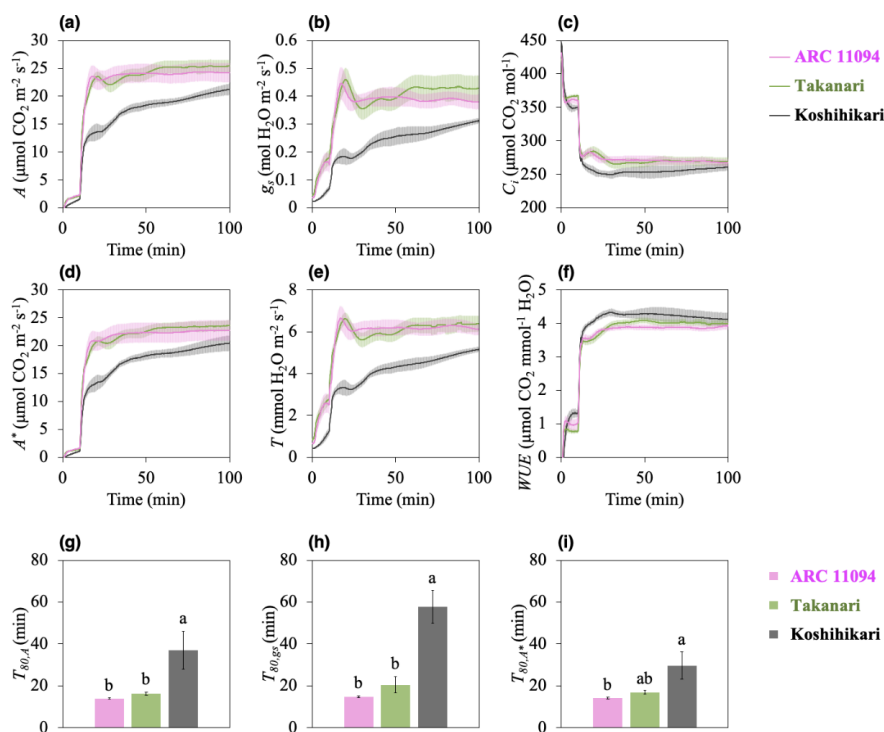


Figure 1 Responses of photosynthetic parameters to changes in light intensity. CO_2 assimilation rate (A : **a**), stomatal conductance (g_s : **b**), intercellular CO_2 concentration (C_i : **c**), normalized CO_2 assimilation rate to a C_i of 250 $\mu\text{mol mol}^{-1}$ (A^* : **d**), transpiration rate (T : **e**) and water use efficiency (WUE : **f**) in ARC 11094 (pink), Takanari (green) and Koshihikari (gray) are shown. These photosynthetic parameters were recorded simultaneously every 10 seconds with LI-6800 at a reference CO_2 concentration of 400 $\mu\text{mol mol}^{-1}$, an air temperature of 30°C and a relative humidity of 55–65%. Time to reach 80% of the maximum values during induction after low light irradiation was calculated in A , g_s and A^* ($T_{80,A}$, T_{80,g_s} and T_{80,A^*} : **g**, **h** and **i**). Values are mean \pm SE ($n = 4-5$). Lower-case letters represent significant differences among genotypes at $P < 0.05$ (Tukey–Kramer multiple comparison test).

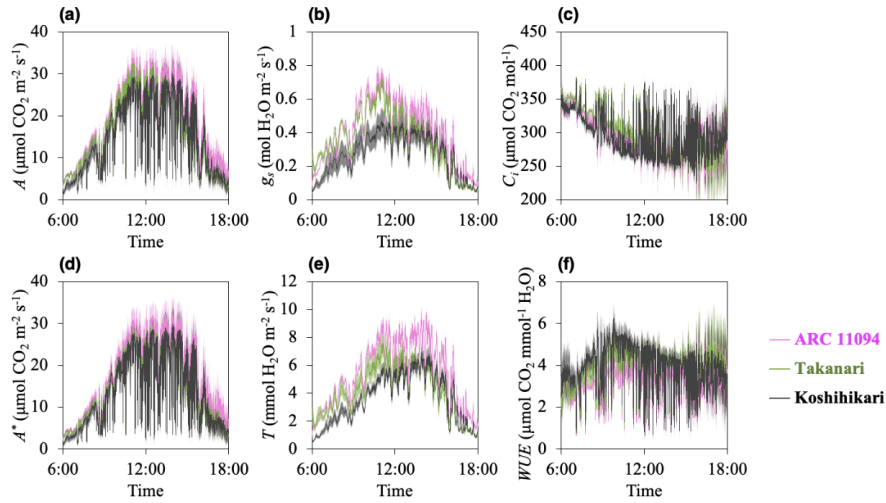


Figure 2 Diurnal changes of photosynthetic parameters under field-mimicked environment. CO_2 assimilation rate (A : **a**), stomatal conductance (g_s : **b**), intercellular CO_2 concentration (C_i : **c**), normalized CO_2 assimilation rate to a C_i of $250 \mu\text{mol mol}^{-1}$ (A^* : **d**), transpiration rate (T : **e**) and water use efficiency (WUE : **f**) in ARC 11094 (pink), Takanari (green) and Koshihikari (gray) are shown. These photosynthetic parameters were recorded simultaneously every 10 seconds for 12 hours with LI-6400, replicating the PPFD and air temperature observed in rice canopy in the leaf chamber at a reference CO_2 concentration of $400 \mu\text{mol mol}^{-1}$. Values are mean \pm SE ($n = 3$).

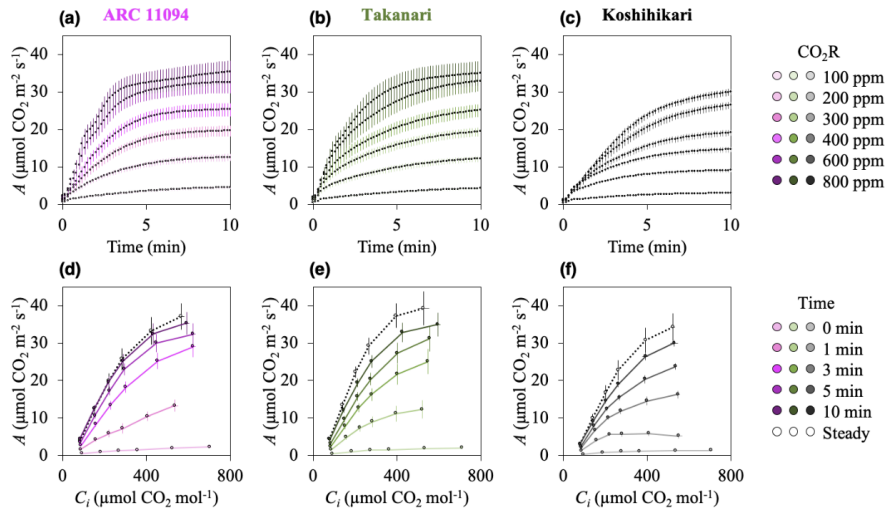


Figure 3 Non-steady state photosynthesis under different CO_2 concentration. Induction response of CO_2 assimilation rate at reference CO_2 concentration of 100, 200, 300, 400, 600 and $800 \mu\text{mol mol}^{-1}$ (**a**, **b** and **c**), and dynamics of $A - C_i$ curve (**d**, **e** and **f**) in ARC 11094 (pink), Takanari (green) and Koshihikari (gray) are shown. Photosynthetic parameters after high light irradiation were recorded every 10 seconds with LI-6800 at an air temperature of 30°C and a relative humidity of 55–65%. $A - C_i$ curve analysis under steady state was conducted independently. Values are mean \pm SE ($n = 4-5$).

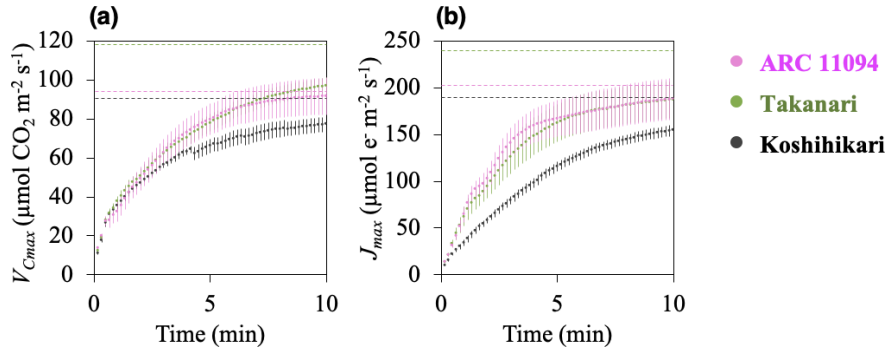


Figure 4 Dynamics of limiting factors in photosynthetic induction. Induction response of the maximum rate of carboxylation (V_{Cmax} : **a**) and electron transport (J_{max} : **b**) in ARC 11094 (pink), Takanari (green) and Koshihikari (gray) are shown. These values were calculated using the data in Figure 4 and normalized to 25°C. Dashed colored lines indicate the values under steady state. Values are mean \pm SE (n = 4–5).

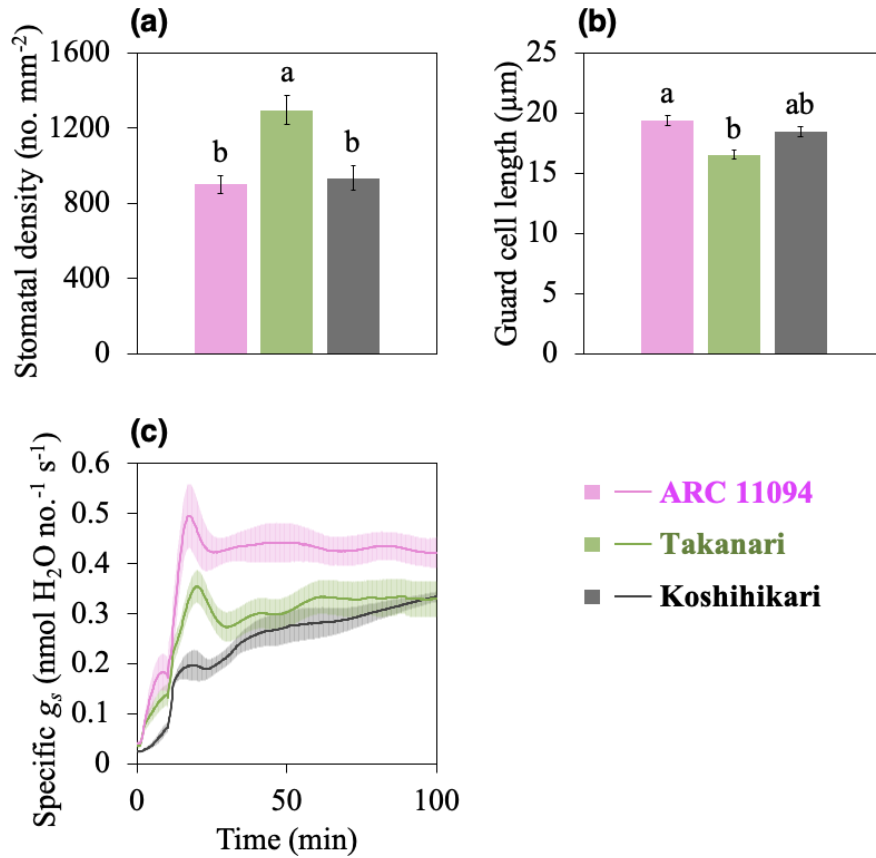


Figure 5 Stomatal morphology and response of specific stomatal conductance to changes in light intensity. Stomatal density (**a**) and guard cell length (**b**), and dynamics of specific stomatal conductance under non-steady state (**c**) in ARC 11094 (pink), Takanari (green) and Koshihikari (gray) are shown. Morphological traits of stomata were evaluated with SUMP method. Specific stomatal conductance was calculated by dividing stomatal conductance, which was obtained from Figure 1, by stomatal density. Values are mean \pm SE (n = 4–5). Lower-case letters represent significant differences among genotypes at $P < 0.05$ (Tukey-

Kramer multiple comparison test).

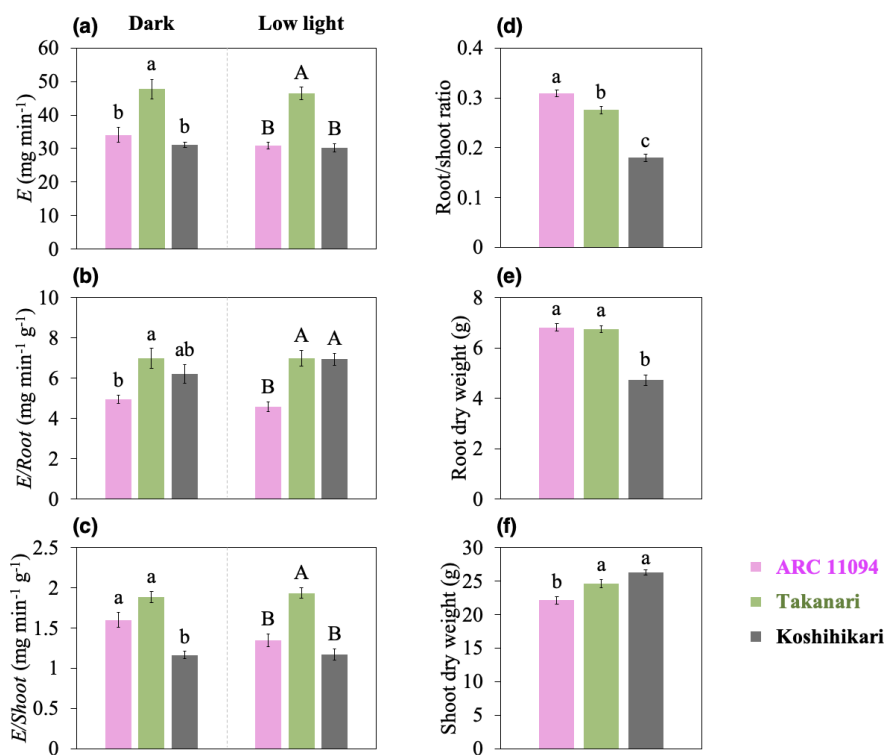


Figure 6 Water uptake of the whole root system. Exudation rate per plant (E : **a**), normalized E to the root or shoot dry weight ($E/Root$: **b**, $E/Shoot$: **c**), root/shoot ratio (**d**) and root or shoot dry weight (**e**, **f**) in ARC 11094 (pink), Takanari (green) and Koshihikari (gray) are shown. Left and right in **a**, **b** and **c** are the values at dark or 10 minutes after light transition from dark to low light intensity ($50 \mu\text{mol photons m}^{-2} \text{s}^{-1}$), respectively. Exudates were collected for 30 minutes after cutting, and then exudation rates were calculated. $E/Root$ and $E/Shoot$ were calculated by dividing E by root or shoot dry weight, respectively. Values are mean \pm SE (**a**, **b** and **c** : $n = 4$, **d**, **e** and **f** : $n = 8$). Letters represent significant differences among genotypes at $P < 0.05$ (Tukey-Kramer multiple comparison test).

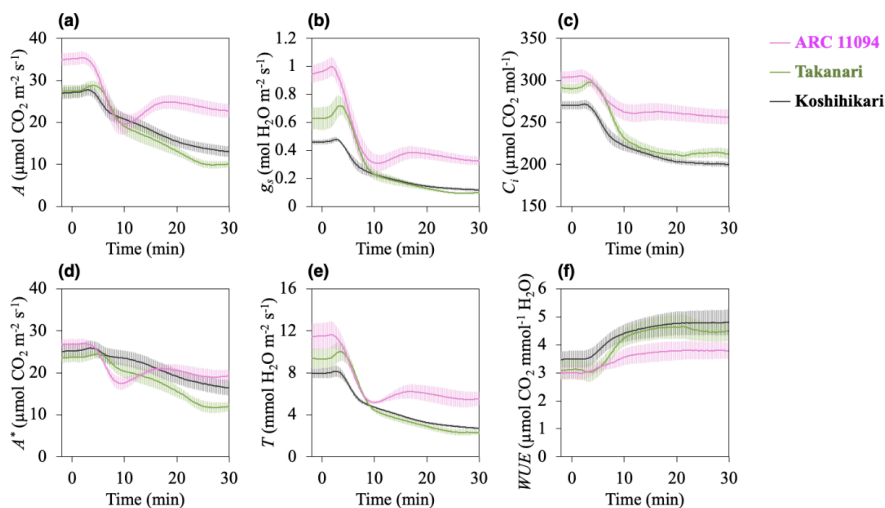


Figure 7 Responses of photosynthetic parameters to changing osmotic potential. CO₂ assimilation rate (A : **a**), stomatal conductance (g_s : **b**), intercellular CO₂ concentration (C_i : **c**), normalized CO₂ assimilation rate to a C_i of 250 $\mu\text{mol mol}^{-1}$ (A^* : **d**), transpiration rate (T : **e**) and water use efficiency (WUE : **f**) in ARC 11094 (pink), Takanari (green) and Koshihikari (gray) are shown. These photosynthetic parameters were recorded simultaneously every 10 seconds with LI-6800 at a PPFD of 1500 $\mu\text{mol photons m}^{-2} \text{s}^{-1}$, a reference CO₂ concentration of 400 $\mu\text{mol mol}^{-1}$, an air temperature of 30°C and a relative humidity of 55–65%. Osmotic potential was changed by adding 1% (w/v) PEG-4000 into the water to set the final concentration of the PEG-4000 to 0.1% (w/v) and stirred gently. Values are mean \pm SE (n = 6).